

Supporting Information

Trigonal columnar self-assembly of bent phasid mesogens

Huifang Cheng,^{‡,a} Ya-xin Li,^{‡,b} Xiang-bing Zeng,^b Hongfei Gao,^a Xiaohong Cheng,^{a,*} Goran Ungar^{b,c,*}

¹ Key Laboratory of Medicinal Chemistry for Natural Resources, Chemistry Department, Yunnan University

² Department of Materials Science and Engineering, University of Sheffield, Sheffield S1 3JD, U.K.

³ Department of Physics, Zhejiang Sci-Tech University, Xiasha College Park, Zhejiang 310018, China

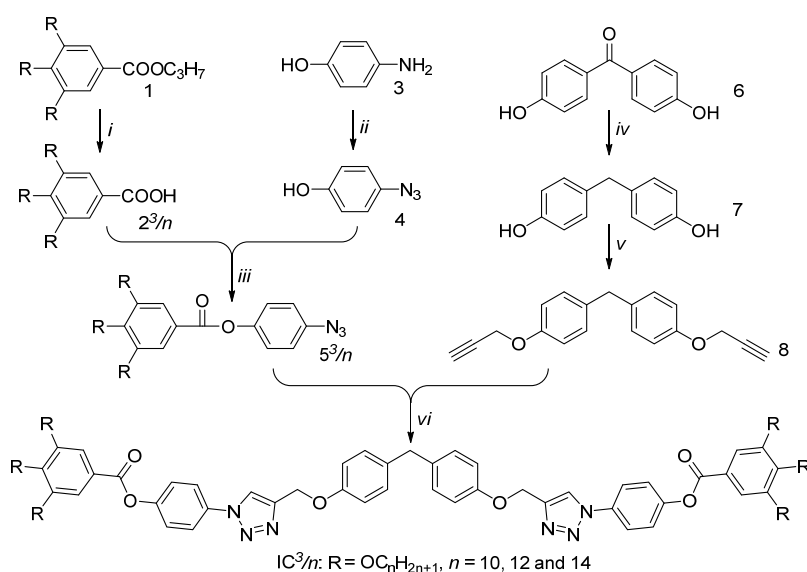
[‡]Both authors contributed equally to this work.

Contents

Synthesis	2
Characterization and Modelling Techniques	5
DSC Results	6
Additional Optical Micrographs	7
Additional X-ray Diffraction Data	8
Estimate of the number of molecules per column stratum	11
Arrangement of columns on substrate surface	11
Additional second harmonic generation data	12
References	12

Synthesis

Reactions requiring an inert gas atmosphere were conducted under argon and the glassware was oven-dried (140 °C). Commercially available chemicals were used as received. ¹H NMR and ¹³C NMR spectra were recorded on a Bruker-DRX-400 spectrometer and Bruker-DRX-500 spectrometer. Elemental analysis was performed using an Elementar VARIO EL elemental analyzer. Column chromatography was performed with merck silica gel 60 (230-400 mesh). The intermediates were purified by column chromatography, their structures were confirmed by ¹H NMR and the purity was checked by TLC. Full analytic characterization was provided for all final compounds. Alkoxybenzoic acid **2^{3/n}** were prepared according to literature procedures.^{S1}



Scheme 1 Synthesis of compounds **IC^{3/n}**. *Reagents and conditions*: i) KOH, CH₃CH₂OH, reflux, over night; ii) a) NaNO₂/HCl, 0 °C, 1 h; b) NaN₃, 0-5 °C, 5 h; iii) dicyclohexylcarbodiimide, 4-dimethylaminopyridine, CH₂Cl₂, 0-5 °C, 18 h; iv) LiAlH₄, AlCl₃, THF, 65 °C, 48 h; v) KOH, propargyl bromide, acetone, reflux; vi) tert-butanol, THF, H₂O, sodium ascorbate, CuSO₄·5H₂O, 25 °C, 20 h.

Synthesis of 4-Azidophenol **4**^{S2}

4-Aminophenol **6** (1.8 g, 16.5 mmol) was suspended in aqueous hydrochloric acid (2 M, 36 mL), the mixture was cooled to 0 °C, and a solution of NaNO₂ (1.37 g, 20 mmol) in water (3 mL) was added. The mixture was stirred for 1 h at 0 °C, then a solution of NaN₃ (1.64 g, 25 mmol) in water (3 mL) was added and stirred for 5 h at 0~5 °C. Water (50 mL) and CH₂Cl₂ (50 mL) were added, the organic layer was separated, the aqueous layer was extracted with CH₂Cl₂ (2 × 30 mL), and the combined organic layer was washed with brine (2 × 20 mL) and dried over anhydrous Na₂SO₄ and the solvent were evaporated in vacuo. The residue was purified by column chromatography (petroleum ether : ethyl acetate = 8 : 1). Yield 1.7 g, 76 %; brownish solid. ¹H NMR (CDCl₃, 500 MHz), δ (ppm): 6.91-6.89 (d, 2 H, J = 7.4 Hz, ArH), 6.83-6.81 (d, 2 H, J = 7.4 Hz, ArH), 5.12 (s, 1 H, ArOH).

General procedure for the synthesis of $5^3/n^{S2}$

Appropriate alkoxybenzoic acid $2^3/n$ (0.6 mmol), 4-azidophenol **4** (0.6 mmol) and DMAP (0.01 mmol) were dissolved in dry CH_2Cl_2 (15 mL). The reaction mixture was cooled down to 0 °C and DCC (0.6 mmol) in CH_2Cl_2 (2 mL) was slowly added. After adding the last portion of DCC the cooling bath was removed and the mixture was stirred at 25 °C for 20 hours. The solid was removed by filtration and the solvent was removed in *vacuo*. The residue was purified by chromatography (petroleum ether/dichloromethane = 8 : 5).

5³/10: Yield: 305 mg, 72 %; light yellow solid. ¹H NMR (CDCl_3 , 500 MHz), δ (ppm): 7.39 (s, 2 H, ArH), 7.20-7.18 (d, 2 H, $J = 8.8$ Hz, ArH), 7.09-7.07 (d, 2 H, $J = 8.8$ Hz, ArH), 4.07-4.03 (m, 6 H, 3 ArOCH₂), 1.86-1.75 (m, 6 H, 3 ArOCH₂CH₂), 1.49-1.26 (m, 42 H, 21 CH₂), 0.90-0.87 (t, 9H, $J = 6.5$ Hz, 3 CH₃).

5³/12: Yield: 385 mg, 81 %; light yellow solid. ¹H NMR (CDCl_3 , 500 MHz), δ (ppm): 7.39 (s, 2 H, ArH), 7.20-7.18 (d, 2 H, $J = 8.8$ Hz, ArH), 7.09-7.07 (d, 2 H, $J = 8.8$ Hz, ArH), 4.07-4.03 (m, 6 H, 3 ArOCH₂), 1.86-1.75 (m, 6 H, 3 ArOCH₂CH₂), 1.49-1.27 (m, 54 H, 27 CH₂), 0.90-0.87 (t, 9 H, $J = 6.5$ Hz, 3 CH₃).

5³/14: Yield: 410 mg, 78 %; light yellow solid. ¹H NMR (CDCl_3 , 500 MHz), δ (ppm): 7.39 (s, 2 H, ArH), 7.20-7.18 (d, 2 H, $J = 8.7$ Hz, ArH), 7.09-7.07 (d, 2 H, $J = 8.7$ Hz, ArH), 4.07-4.03 (m, 6 H, 3 ArOCH₂), 1.84-1.75 (m, 6 H, 3 ArOCH₂CH₂), 1.49-1.26 (m, 66 H, 33 CH₂), 0.89-0.87 (t, 9 H, $J = 6.5$ Hz, 3 CH₃).

Synthesis of 4,4'-dihydroxydiphenylmethane **7**^{S3}

Compound 4,4-dihydroxybenzophenone **6** (1 g, 4.67 mmol), LiAlH_4 and AlCl_3 were dissolved in dry THF (80 mL). The mixture was stirred 48 h at 65 °C. The solvent was removed in *vacuo*. The residue was extracted with ethyl acetate (2 × 30 mL). The combined extracts were washed with brine (2 × 20 mL), dried over anhydrous Na_2SO_4 , then the solvent was removed in *vacuo*. The residue was purified by chromatography (petroleum ether/ethyl acetate = 3 : 1). Yield: 635 mg, 68%, white solid. ¹H NMR (CDCl_3 , 400 MHz), δ (ppm): 7.04-7.02 (d, 4 H, $J = 8.4$ Hz, ArH), 6.76-6.74 (d, 4 H, $J = 8.4$ Hz, ArH), 4.59 (s, 2 H, ArOH), 3.84 (s, 2 H, ArCH₂Ar).

Synthesis of compound **8**

Compound 4,4'-dihydroxydiphenylmethane **7** (400 mg, 2.0 mmol), propargyl bromide (708 mg, 6.0 mmol) and KOH (448 mg, 8.0 mmol) were dissolved in dry acetone (10 mL) under a nitrogen atmosphere. The mixture was refluxed over night. The solvent was removed in *vacuo*. The residue was extracted with ethyl acetate (2 × 30 mL). The combined extracts were washed with brine (2 × 20 mL), dried over anhydrous Na_2SO_4 , then the solvent was removed in *vacuo*. The residue was purified by chromatography (petroleum ether/ethyl acetate = 10 : 1). Yield: 486 mg, 88%, light yellow liquid. ¹H NMR (CDCl_3 , 400 MHz), δ (ppm): 7.13-7.10 (m, 4 H, ArH), 6.92-6.89 (m, 4 H, ArH), 4.68-4.66 (m, 4 H, ArOCH₂), 3.89-3.88 (d, 2 H, $J = 3.2$ Hz, ArCH₂Ar), 2.53-2.51 (m, 2 H, alkyne-H).

General procedure for the synthesis of IC^{3/n}

Compound 5^{3/n} (0.20 mmol), compound 8 (0.085 mmol) were dissolved in dry THF (8 mL), tert-butyl alcohol: H₂O = 1 : 1 (2 mL), CuSO₄·5H₂O (0.062 mmol) and sodium ascorbate (0.114 mmol) were added. The mixture was stirred over night at 45°C. The solvent was removed in *vacuo*. The residue was extracted with CH₂Cl₂ (3 × 30 mL). The combined extracts were washed with brine (2 × 20 mL), dried over MgSO₄, then the solvent was removed in *vacuo*. The residue was purified by chromatography (CH₂Cl₂: ethyl acetate = 60 : 1).

IC^{3/10}: Yield: 130 mg, 90%, white solid. ¹H NMR (CDCl₃, 400 MHz), δ (ppm): 8.05 (s, 2 H, triazole-H), 7.81-7.79 (d, 4 H, *J* = 8.8 Hz, ArH), 7.41 (s, 4 H, ArH), 7.38-7.36 (d, 4 H, *J* = 8.8 Hz, ArH), 7.13-7.11 (d, 4 H, *J* = 8.8 Hz, ArH), 6.96-6.94 (d, 4 H, *J* = 8.8 Hz, ArH), 5.28 (s, 4 H, ArOCH₂-triazole), 4.09-4.03 (m, 12 H, 6 ArOCH₂), 3.89 (s, 2 H, ArCH₂Ar), 1.87-1.73 (m, 12 H, 6 ArOCH₂CH₂), 1.49-1.47 (m, 12 H, 6 ArOCH₂CH₂CH₂), 1.28 (s, 72 H, 36 CH₂), 0.89-0.86 (m, 18 H, 6 CH₃); ¹³C NMR (CDCl₃, 100 MHz), δ (ppm): 164.86(1C), 156.66(1C), 153.15(2C), 151.24(1C), 145.44(1C), 143.44(1C), 134.67(1C), 134.46(1C), 130.02(2C), 123.38(2C), 121.87(2C), 121.09(2C), 114.89(2C), 108.75(2C), 73.74(2C), 69.42(4C), 62.20(2C), 40.27(1C), 32.06, 30.47, 29.81, 29.75, 29.51, 29.42, 26.21, 22.81, 14.22 (multi carbons in alkyl chain); Elemental Analysis calcd (%) for C₁₀₅H₁₅₄N₆O₁₂ (1691.16): C 74.52, H 9.17, N 4.97; found: C 74.50, H 9.16, N 4.98.

IC^{3/12}: Yield: 140 mg, 89%, white solid. ¹H NMR (CDCl₃, 400 MHz), δ (ppm): 8.05 (s, 2 H, triazole-H), 7.82-7.79 (m, 4 H, ArH), 7.41 (s, 4 H, ArH), 7.39-7.36 (m, 4 H, ArH), 7.13-7.11 (d, 4 H, *J* = 8.8 Hz, ArH), 6.96-6.94 (d, 4 H, *J* = 8.8 Hz, ArH), 5.28 (s, 4 H, ArOCH₂-triazole), 4.09-4.03 (m, 12 H, 6 ArOCH₂), 3.89 (s, 2 H, ArCH₂Ar), 1.87-1.75 (m, 12 H, 6 ArOCH₂CH₂), 1.51-1.47 (m, 12 H, 6 ArOCH₂CH₂CH₂), 1.26 (s, 96 H, 48 CH₂), 0.89-0.86 (m, 18 H, 6 CH₃). ¹³C NMR (CDCl₃, 100 MHz), δ (ppm): 164.87(1C), 156.68(1C), 153.16(2C), 151.20(1C), 145.44(1C), 143.49(1C), 134.67(1C), 134.48(1C), 130.02(2C), 121.90(3C), 121.05(2C), 120.53(1C), 114.91(2C), 108.79(2C), 73.75(2C), 69.45(4C), 62.25(2C), 40.27(1C), 32.04, 30.47, 29.81, 29.75, 29.51, 29.42, 26.21, 22.81, 14.22 (multi carbons in alkyl chain); Elemental Analysis calcd (%) for C₁₁₇H₁₇₈N₆O₁₂ (1859.35): C 75.52, H 9.64, N 4.52; found: C 75.50, H 9.63, N 4.51.

IC^{3/14}: Yield: 159 mg, 92%, white solid. ¹H NMR (CDCl₃, 400 MHz), δ (ppm): 8.05 (s, 2 H, triazole-H), 7.81-7.79 (d, 4 H, *J* = 9.2 Hz, ArH), 7.41 (s, 4 H, ArH), 7.38-7.36 (d, 4 H, *J* = 8.8 Hz, ArH), 7.13-7.11 (d, 4 H, *J* = 8.4 Hz, ArH), 6.96-6.94 (d, 4 H, *J* = 8.8 Hz, ArH), 5.28 (s, 4 H, ArOCH₂-triazole), 4.09-4.03 (m, 12 H, 6 ArOCH₂), 3.89 (s, 2 H, ArCH₂Ar), 1.87-1.73 (m, 12 H, 6 ArOCH₂CH₂), 1.51-1.45 (m, 12 H, 6 ArOCH₂CH₂CH₂), 1.26 (s, 120 H, 60 CH₂), 0.89-0.86 (m, 18 H, 6 CH₃); ¹³C NMR (CDCl₃, 100 MHz), δ (ppm): 164.81(1C), 156.64(1C), 153.12(2C), 151.22(1C), 145.39(1C), 143.46(1C), 134.63(1C), 134.43(1C), 129.98(2C), 123.33(3C), 121.84(2C), 121.00(1C), 114.87(2C), 108.76(2C), 73.70(2C), 69.41(4C), 62.21(2C), 40.23(1C), 32.00, 30.43, 29.77, 29.71, 29.44, 29.38, 26.16, 22.76, 14.17 (multi carbons in alkyl chain); Elemental Analysis calcd (%) for C₁₂₉H₂₀₂N₆O₁₂ (2027.54): C 76.36, H 10.03, N 4.14; found: C 76.34, H 10.02, N 4.13.

Characterization and Modelling Techniques

DSC thermograms were recorded on a DSC 200 F3 Maia calorimeter (NETZSCH) instrument with heating/cooling rates as specified. Optical micrographs with crossed polarizers were recorded using an Olympus BX1 microscope equipped with Mettler hot stage.

GISAXS experiments were carried out at BM28 at European Synchrotron Radiation Facility, France. The X-ray energy was 12.0 keV, and the 2d diffractograms were collected using a MAR165 CCD camera. Thin film samples were prepared from melt on silicon substrate. *n*-tetracontane was used to calibrate the sample to detector distance. **Powder SAXS and WAXS** experiments were done at station I22 of Diamond Light Source, U.K. Powder samples were prepared in 1 mm glass capillaries and held in a modified Linkam hot stage. Pilatus 2M detector (Dectris) at a distance of 2.2 m from the sample was used. The X-ray energy was 12.4 keV. **Preliminary SAXS** patterns were recorded on a Xenocs system based at Zhejiang Sci-Tech University consisting of a microspot Cu-K α X-ray generator, an infinity focusing multilayer 3D-curved mirror, scatterless slits collimator, and a MAR Research 345 image plate detector. **Electron density maps** were calculated by inverse Fourier transformation using the standard procedure as described in International Tables for Crystallography. The choice of phase is discussed in the text.

Samples of ca. 50 μm thickness for frequency-doubled light emission, or **second harmonic generation** (SHG) measurements were prepared on the rough side of silicon wafer and examined using a Zeiss LSM 510 Meta upright laser-scanning confocal microscope (Oberkochen, Germany) with a 40X/0.75NA objective. Temperature was controlled by a Linkam hot stage. A Chameleon Ti:Sapphire femtosecond pulsed laser (Coherent, California, USA) tuned to 800 nm, was attached to the microscope and focused onto the sample resulting in a SHG signal detectable at 400 nm. In order to exclude possible surface effects, first the beam was focused at the bottom of the LC film in contact with the Si substrate, then at 10 μm , 20 μm and sometimes 30 μm height. The SHG ratio was calculated by dividing the intensities at 400 nm by the averaged background around the peak. The normalized 400 nm signal for **IC³/12** and **IC³/14**, collected 20 μm above the substrate, is shown as a function of temperature in Figure 3a. Measurements are made on very slow cooling from the isotropic phase. The sharp increase in the signal below the isotropization temperature confirms that the columnar LC phase that forms at that temperature lacks centre of inversion. Diagrams that also include the measurements at 0 and 10 μm height are shown in Figure S10.

Molecular models were built using Materials Studio (Accelrys). Geometry optimization and molecular dynamic simulation were performed using the Forcite Plus module with Universal Force Field. The experimental value for *a*-parameter and the value for *c* from Table S4 were used. The convergence tolerances for geometry optimization were 0.001 kcal/mol for energy and 0.5 kcal/mol/Å for force. NVT annealing dynamics was performed through 30 cycles between 300 and 600 K. with a total annealing time of 30 ps. The MD annealing was performed in a “supercell” box with periodic boundary conditions containing 9 unit cells.

DSC Results

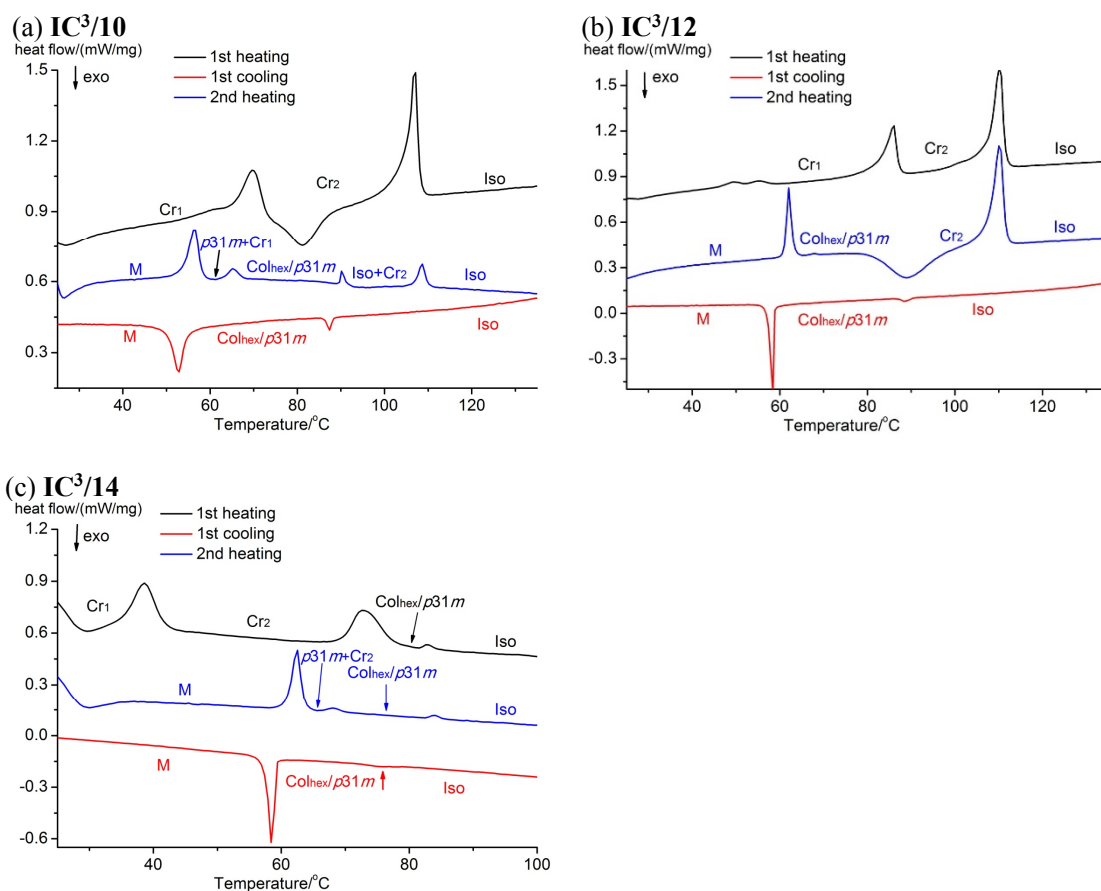


Figure S1 DSC thermograms of compounds IC³/*n* at heating and cooling scan rate of 5 K min⁻¹.

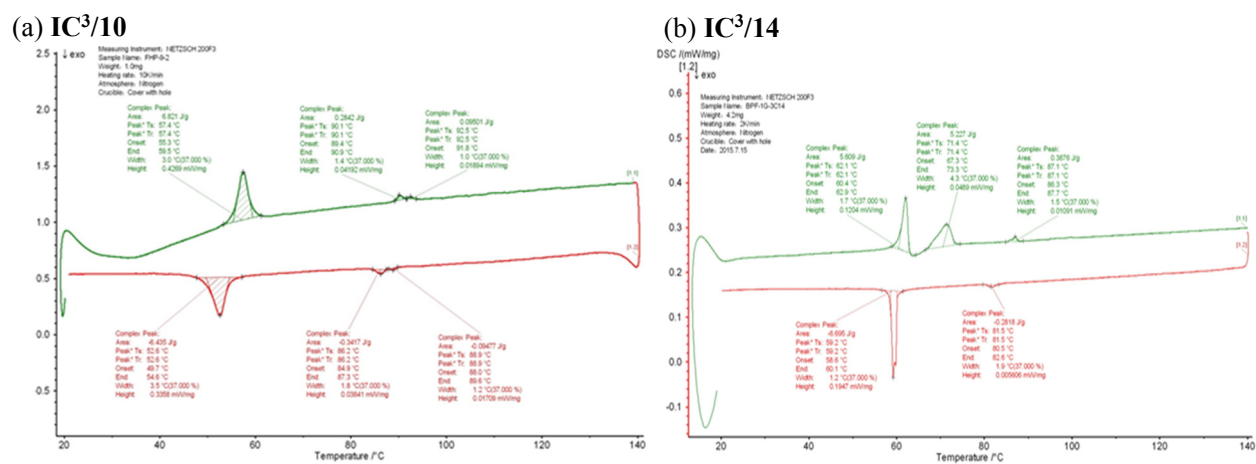


Figure S2 DSC cooling and 2nd heating scans of (a) IC³/10 at 10 K min⁻¹, and (b) IC³/14 at 2 K min⁻¹.

Additional Optical Micrographs

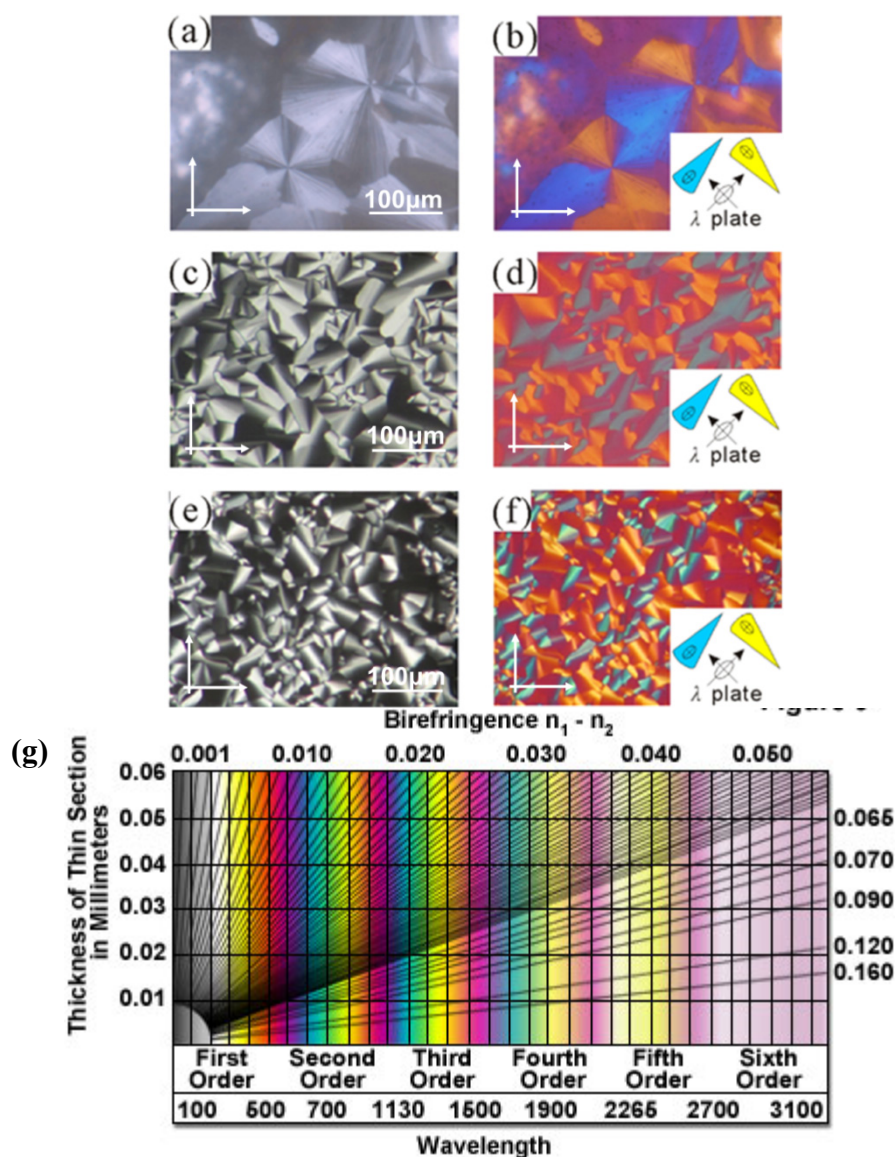


Figure S3 Polarized optical microscopy textures of (a, b) $\text{IC}^3/10$ at 90°C , (c, d) $\text{IC}^3/12$ at 77°C and (e, f) $\text{IC}^3/14$ at 70°C . (b,d,f) are recorded with a full-wave (λ) plate. (g) Michel-Levy colour chart (<http://www.olympusmicro.com/primer/techniques/polarized/michel.html>).

Determination of the direction of the slow (high refractive index) axis was based on the fact that by adding a fixed retardation to the whole image using a λ -plate, positive and negative phase shifts $+\Delta\Gamma$ and $-\Delta\Gamma$ between the ordinary and extraordinary rays could be distinguished. The λ -plate we used added a retardation of exactly 2π in the green (530 nm), so what appears black without the plate becomes magenta (white minus green – see the Michel-Levy chart in Figure S3g). In areas with positive retardation parallel to the slow axis of the λ -plate the retardation is added, making the colour blue (phase difference $2\pi+\Delta\Gamma$), while in areas where retardation was subtracted the colour is yellow (phase difference $2\pi-\Delta\Gamma$). Thus e.g. in the blue sectors of the “spherulites” the slow axis of the LC is southwest-to-northeast, while the column direction is southeast-to-northwest (columns circle around the “spherulite” – see ref. S4). Thus the slow axis, i.e. the long axis of the aromatic core of the molecules, is perpendicular to the columns.

Additional X-ray Diffraction Data

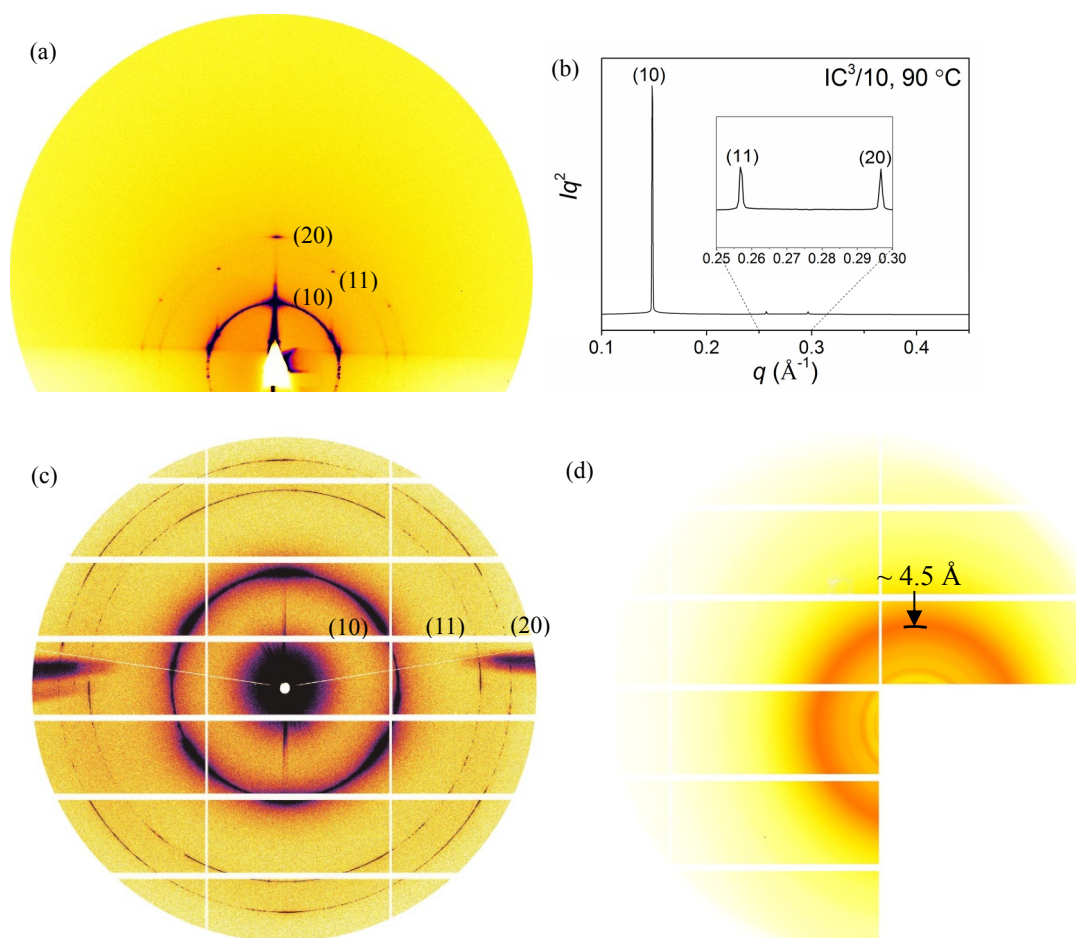


Figure S4. X-ray diffraction patterns of the Col/p31m phase in IC³/10. (a) GISAXS pattern recorded at 90 °C; (b) azimuthally averaged Lorentz-corrected profile of the transmission powder SAXS pattern in (c); 2D SAXS powder pattern recorded at 90 °C; (d), WAXS pattern recorded simultaneously with the SAXS pattern in (c). The vertical and horizontal white lines in (c, d) are the gaps between the detector elements. The missing rectangular section in (d) is the position of the SAXS detector. The diffuse outer ring in (d) with maximum at around 4.5 Å arises from interaction between both alkyl chains and between aromatic rings at adjacent strata. The sharper inner ring comes from scattering on Kapton window.

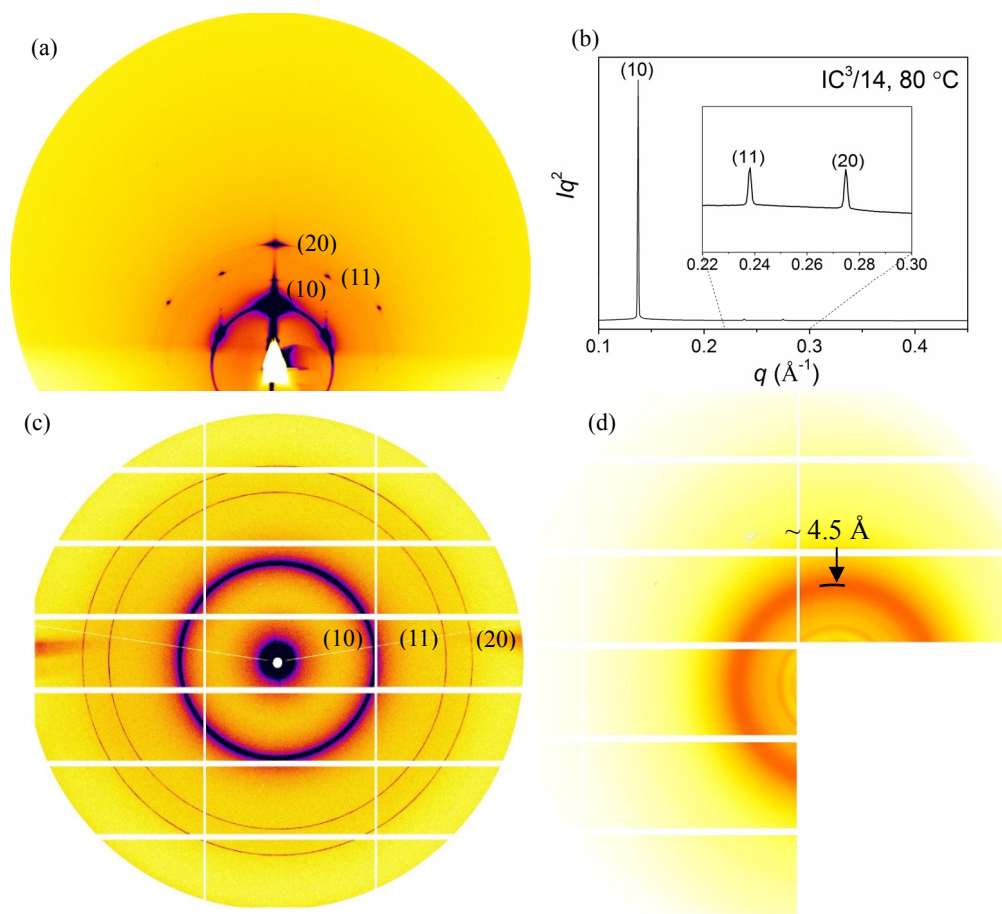


Figure S5. X-ray diffraction patterns of the Col/*p31m* phase in IC³/14. Description of panels (a)-(d) is as for Figure S4.

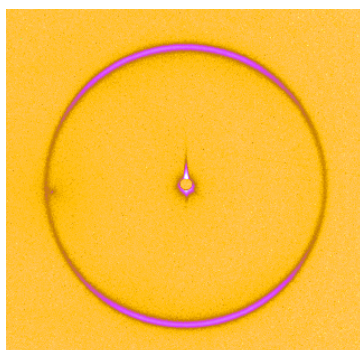


Figure S6. Transmission SAXS pattern of IC³/14 held in glass capillary recorded at 90°C. Capillary axis is horizontal. Only the inner ring (10) is shown. Preferred orientation of the columns parallel to the capillary axis is visible.

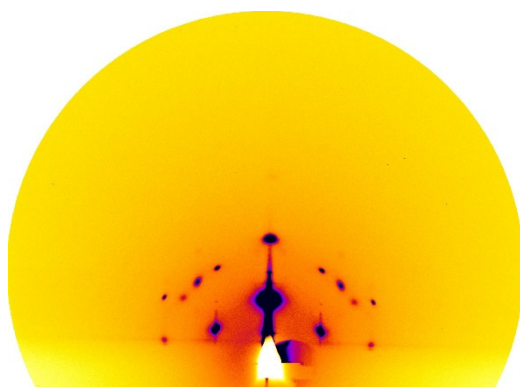


Figure S7. GISAXS pattern of the M-phase in IC³/12 cooled from the isotropic liquid to 50 °C.

Table S1 The indices, experimental, calculated *d*-spacings, intensities and lattice parameter of IC³/10 obtained from SAXS at 90 °C. All intensity values are Lorentz and multiplicity corrected.

(hk)	<i>d</i> -spacing (nm) experimental	<i>d</i> -spacing (nm) calculated	<i>Intensity</i>
(10)	4.25	4.24	23.7
(11)	2.44	2.45	0.148
(20)	2.12	2.12	0.0791
<i>a</i> = 4.89 nm			

Table S2 The indices, observed, calculated *d*-spacings, intensities and lattice parameter of IC³/12 obtained from SAXS at 80 °C. All intensity values are Lorentz and multiplicity corrected.

(hk)	<i>d</i> -spacing (nm) experimental	<i>d</i> -spacing (nm) calculated	<i>Intensity</i>	<i>Phase angle</i> (°)
(10)	4.46	4.45	27.7	0
(11)	2.56	2.57	0.272	120
(20)	2.22	2.22	0.217	180
<i>a</i> = 5.13 nm				

Table S3 The indices, experimental, calculated *d*-spacings, intensities and lattice parameter of IC³/14 obtained from SAXS at 80 °C. All intensity values are Lorentz and multiplicity corrected.

(hk)	<i>d</i> -spacing (nm) experimental	<i>d</i> -spacing (nm) calculated	<i>Intensity</i>
(10)	4.59	4.58	14.6
(11)	2.64	2.64	0.0655
(20)	2.29	2.29	0.0672
<i>a</i> = 5.28 nm			

Electron density maps as a function of the phase angle ϕ of reflection (11)

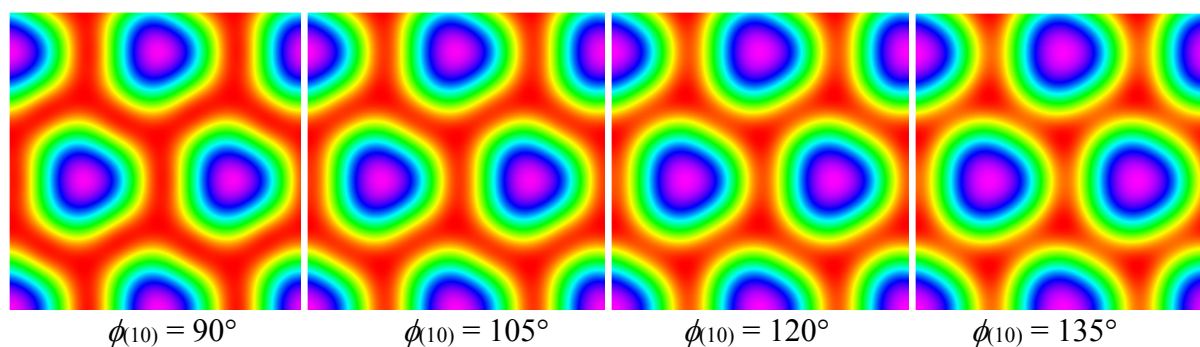


Figure S8 Electron density maps of the $p31m$ columnar phase of compound **IC³/12** using different values of $\phi_{(10)}$.

Estimate of the number of molecules per column stratum

Table S4 Estimation of the height of a stratum c assuming $n = 3$ molecules per unit cell (column stratum)

Compound	V_{arom} (nm ³) ^a	V_{aliph} (nm ³) ^b	V_{mol} (nm ³) ^c	V_{cell} (nm ³) ($n = 3$)	A (nm ²) ^d	c (nm) ($n = 3$)
IC³/10	0.98	2.01	2.99	8.99	20.7	0.434
IC³/12	0.98	2.40	3.38	10.14	22.8	0.445
IC³/14	0.98	2.80	3.78	11.34	24.1	0.471

a: V_{arom} = Volume of aromatic part of the molecule calculated using the crystal volume increments.^{S4}

b: V_{aliph} = Volume of aliphatic part of the molecule assuming a density of 0.8 g/cm³.

c: Volume of molecule ($V_{\text{mol}} = V_{\text{arom}} + V_{\text{aliph}}$);

d: Cross section area of a unit cell of hexagonal phase $A = a^2 * 3^{1/2}/2$

e: $c = V_{\text{cell}}/A$

Arrangement of columns on substrate surface

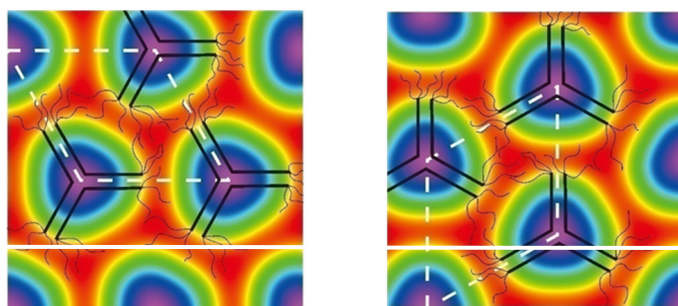


Figure S9 Two possible orientations of the hexagonal lattice of columns on a horizontal silicon substrate surface – view along column axis. The GISAXS patterns in Figures 2b, S4a and S5a all show that the $\text{Col}_{\text{hex}}/p31m$ phase in **IC³/ n** compounds faces the substrate with its (100) face (figure on the left) rather than its (110) face (figure on the right). This is the usual case in columnar phases with planar anchoring (ref 21). The horizontal white line suggests how the column array might face the substrate, showing that the columns would have to be cut through in the (110) arrangement (right). It should also be noted that the columns are surrounded by flexible alkyl chains, which reduces the effect of the shape of the column core, as the cores are not in direct contact with the substrate. Even so, there is bound to be a degree of surface reconstruction in the layer in direct contact with the substrate.

Additional second harmonic generation data

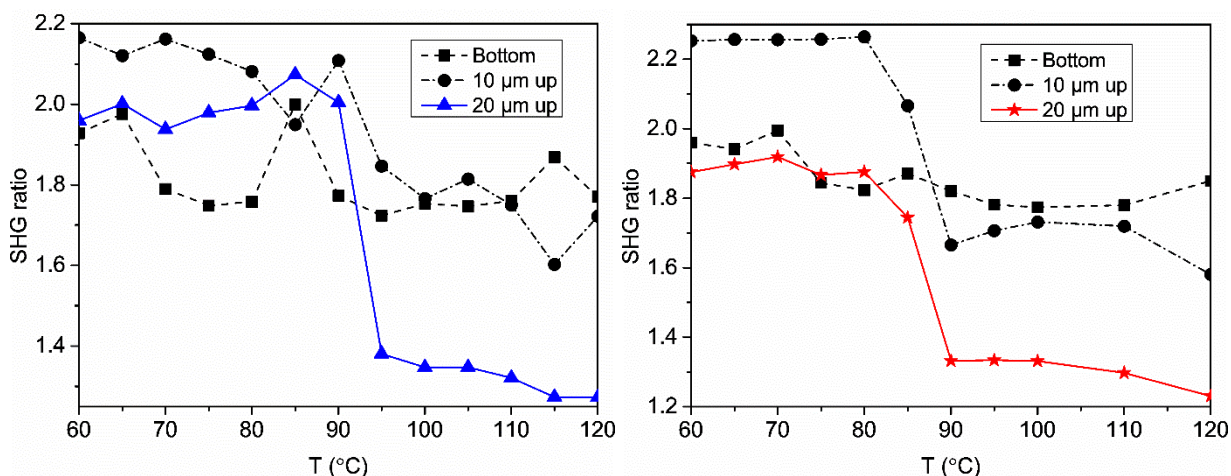


Figure S10 Normalized second harmonic (400 nm) intensity as a function of temperature for IC³/12 (left) and IC³/14 (right) sampled at the LC-Si interface (squares), 10 μm above it (circles) and 20 μm above it (blue triangles for IC³/12 and red stars for IC³/14). The large step-up in SHG signal for the bulk LC coincides with the transition from isotropic liquid to the trigonal phase Col_{hex}/p31m.

References

-
- S1 X. H. Cheng, X. Q. Bai, S. Jing, H. Ebert, M. Prehm, C. Tschierske. *Chem. Eur. J.*, 2010, **16**, 4588–4601.
- S2 X. Tan, L. Kong, H. Dai, X. Cheng, F. Liu and C. Tschierske, *Chem. Eur. J.*, 2013, **19**, 16303-16313.
- S3 A. K. Boal and V. M. Rotello, *J. Am. Chem. Soc.*, 2002, **124**, 5019-5024.
- S4 Immirzi, A.; Perini, B. *Acta Crystallogr. Sect. A*, 1977, **33**, 216.
- S4 Bouligand, Y. *J. Physique*, 1980, **41**, 1297.